How do treadmill speed and terrain visibility influence neuromuscular control of guinea fowl locomotion?

Joanne C. Gordon, Jeffery W. Rankin and Monica A. Daley

Structure and Motion Laboratory, Royal Veterinary College, Hawkshead Lane, Hatfield, Hertfordshire, UK

Abstract

Locomotor control mechanisms must flexibly adapt to both anticipated and unexpected terrain changes to maintain movement and avoid a fall. Recent studies revealed that ground birds alter movement in advance of overground obstacles, but not treadmill obstacles, suggesting context-dependent shifts in use of anticipatory control. We hypothesized that differences between overground and treadmill obstacle negotiation relate to differences in visual sensory information, which influence the ability to execute anticipatory manoeuvres. We explored two possible explanations: 1) previous treadmill obstacles may have been visually imperceptible, as they were low contrast to the tread, and 2) treadmill obstacles are visible for a shorter time compared to runway obstacles, limiting time available for visuomotor adjustments. To investigate these factors, we measured electromyographic activity in 8 hindlimb muscles of the guinea fowl (*Numida meleagris*, n = 6) during treadmill locomotion at two speeds ($0.7 ms^{-1}$ and $1.3 ms^{-1}$) and three terrain conditions at each speed: (i) level, (ii) repeated 5cm low contrast obstacles (<10% contrast, black/black), and (iii) repeated 5cm high contrast obstacles (>90% contrast, black/white). We hypothesized that anticipatory changes in muscle activity would be higher for 1) high contrast obstacles, and 2) the slower treadmill speed, when obstacle viewing time is longer. We found that treadmill speed significantly influenced obstacle negotiation strategy, but obstacle contrast did not. At the slower speed, we observed earlier and larger anticipatory increases in muscle activity and shifts in kinematic timing. We discuss possible visuomotor explanations for the observed context-dependent use of anticipatory strategies.

Introduction

Legged animals navigate complex terrain by flexibly integrating multiple sensory modalities in a hierarchically organized control system that includes short-latency spinal reflexes, rhythmic spinal networks and higher central input via the motor cortex and descending pathways (Dickinson et al., 2000; Pearson, 2000; Nishikawa et al., 2007; Prochazka and Ellaway, 2012). To manoeuvre through changing terrain, motor control must be adapted through both *anticipatory* and *reactionary* mechanisms (Yakovenko et al., 2005; Marigold and Patla, 2007; Donelan et al., 2009). Here we define *anticipatory* control as motor output generated prior to a goal-directed movement, originating from higher brain centers based on an internal predictive model and transmitted via descending spinal pathways (Pearson, 2000; Yakovenko et al., 2004; Frigon and Rossignol, 2006). Sensory information does feed into anticipatory control, but *primarily acts upstream* of spinal networks in the selection, planning and initiation of behaviour in the higher central nervous system (Patla, 1998; Marigold and Patla, 2007; Fajen et al., 2013).

In contrast, we define *reactionary* control as feedback modulation of motor output following limb contact with the terrain, resulting from deviations between anticipated and actual dynamics, predominantly coordinated via short-latency reflex feedback to spinal networks (Moritz and Farley, 2005; Daley et al., 2009). The reactionary response to a perturbation represents a combination of intrinsic limb dynamics in response to terrain contact, and sensory feedback relaying the errors between anticipated and perceived body states (Zehr and Stein, 1999; Moritz and Farley, 2004; Ross and Nichols, 2009). Thus, an interplay occurs between anticipatory and reactionary control mechanisms, because reactionary responses depend on the extent to which anticipatory control has adjusted limb trajectory, posture and impedance appropriately in advance of contact with terrain.

When adequate sensory information is available, anticipatory control should allow animals to optimize movement for the task and environment, to facilitate economic and robust locomotion (Cinelli and Patla, 2008; da Silva et al., 2011; Matthis and Fajen, 2014). We expect animals to use anticipation when possible, because accurate forward planning may improve foot and limb positioning which could maximize stability and minimize energy cost (Matthis and Fajen, 2013). When terrain is uneven and unpredictable, gait is more variable and energy costs increase markedly

(Voloshina et al., 2013). Anticipatory control of limb trajectory may allow animals to move in ways that minimize muscle work and force, minimizing muscular effort, as recently suggested by simulation studies (Birn-Jeffery et al. 2014; Van Why et al. 2014). Nonetheless, reactionary mechanisms are likely of similar importance in locomotion, buffering against unexpected perturbations when visual information is insufficient to accurately anticipate terrain conditions (Moritz and Farley, 2004; Daley and Biewener, 2011).

Recent research suggests ground birds vary their use of anticipatory strategies when negotiating uneven terrain between overground and treadmill conditions. Birds negotiating obstacles overground use anticipatory manoeuvres to vault upwards onto obstacles to avoid excessively crouched postures on the obstacle (Birn-Jeffery, 2012; Birn-Jeffery and Daley, 2012; Birn-Jeffery et al., 2014). In contrast, guinea fowl running over camouflaged obstacles on a treadmill do not use anticipatory strategies, exhibiting pre-obstacle dynamics similar to level terrain (Daley and Biewener, 2011). Instead, birds land with a crouched posture on obstacles, subsequently recovering through posture-dependent changes to muscle force and work (Daley and Biewener, 2011). Given that guinea fowl use anticipatory strategies for overground obstacles, even at high running speeds ($4ms^{-1}$ and higher) (Birn-Jeffery, 2012; Birn-Jeffery and Daley, 2012; Birn-Jeffery et al., 2014), it is unclear why anticipatory strategies were not used in treadmill obstacle negotiation, especially considering the repetitive nature of terrain presentation.

We hypothesize that the difference in obstacle negotiation strategies between overground and treadmill settings relates to differences in visual sensory information, which influence the ability to effectively execute anticipatory manoeuvres. While multiple sensory, dynamic and neuromuscular factors could explain the context-dependent use of anticipatory control (Muller et al., 2010; Belmonti et al., 2013; Matthis and Fajen, 2013; Birn-Jeffery et al., 2014), vision is the most prominent sensory differences between the experiments described above. Human studies have demonstrated that visual perception plays a central role in safe and efficient anticipatory route planning through complex terrain (Hollands et al., 2002; Patla et al., 2002; Mohagheghi et al., 2004; Marigold and Patla, 2008; Matthis and Fajen, 2013). There are three important ways that overground conditions provide greater visual information compared to a treadmill: 1) optical flow is reduced on a treadmill,

minimising visual stimulus compared to overground, 2) obstacles are visible for a longer approach distance in overground locomotion, allowing longer viewing time for anticipatory visuomotor adjustments and 3) treadmill obstacles may have been visually imperceptible due to low contrast to the substrate (<10% contrast) and uniform lighting, particularly in the study design of Daley and Biewener (2011).

On treadmills, the short time between obstacle appearance on the belt and the obstacle encounter, which is approximately 1 stride, may restrict anticipatory control due to visuomotor latencies. In humans, the time available for terrain assessment and visuomotor response is a critical factor in the use of anticipatory strategies (Patla, 1997; Patla and Vickers, 2003). Time available for visual assessment of terrain specifically influences steering, path planning and foot-placement behaviour during walking in cats and humans (Patla, 1997; Fowler and Sherk, 2003). Walking humans target gaze two steps ahead, creating a minimum visuomotor response time of two step periods, which allows them to maintain speed and stability compared to conditions with limited vision (Patla, 1997; Marigold and Patla, 2007; Matthis and Fajen, 2013). Estimates of gaze distance and minimal visuomotor response time have not been studied in birds, to our knowledge. However, treadmills can restrict terrain viewing time to 1 step period or less, by restricting gaze to the short length of the treadmill belt. If birds, like humans and cats, normally gaze 2 steps ahead, visually mediated anticipatory control may be particularly restricted at higher treadmill speeds, when the terrain appears a very short time before it is encountered.

The goal of this study is to investigate the effects of 1) terrain visibility (high/low contrast) and 2) treadmill speed on the neuromuscular control strategies used by guinea fowl during obstacle negotiation. We recorded obstacle negotiation at two treadmill speeds, 0.7ms^{-1} and 1.3ms^{-1}, with the obstacle at the same fixed distance apart at both speeds. At the slower speed, the bird has a longer time between obstacle appearance at the front of the treadmill belt and its encounter in the middle of the treadmill. Additionally, we manipulated the strength of the terrain visual stimulus by using two different obstacle conditions: low contrast obstacles (<10% contrast, black/black), and high contrast obstacles (>90% contrast, black/white). These conditions were selected to investigate whether low obstacle visibility or speed-effects on obstacle viewing time contributed to the lack of observed anticipatory control strategies in the previous study of guinea fowl negotiating treadmill obstacles (Daley

and Biewener, 2011). We used a treadmill experimental setup because running speed of animals cannot be easily controlled in overground settings.

We hypothesize that use of anticipatory control strategies for obstacle negotiation will be greater for (1) high contrast obstacles and (2) at the slower treadmill speed, when obstacle viewing times are longer. Anticipatory control should manifest as larger shifts in muscle activity and gait kinematics in strides preceding foot contact with the obstacle, when compared to level-terrain locomotion at the same speed. At higher speeds, obstacles will be visible on the belt for a shorter time before their encounter, which may restrict visuomotor responses. We therefore expected the greatest anticipatory effects to be observed during trials with high contrast obstacles and slower speed. If we observe no anticipatory control for treadmill obstacle negotiation across all measured conditions, this would suggest a fundamental difference in neuromuscular control between treadmill and overground locomotion, possibly due to sensory differences such as reduced optical flow.

Results

We report electromyographic (EMG) activity from 8 hindlimb muscles spanning a proximo-distal distribution (**Fig. 1, Tab. 1**), recorded using indwelling electrodes (see Methods). Trials were recorded for two speeds ($0.7ms^{-1}$ and $1.3ms^{-1}$) and three terrain conditions at each speed: (i) level, (ii) repeated 5cm low contrast obstacles (<10% contrast, black/black), and (iii) repeated 5cm high contrast obstacles (>90% contrast, black/white). We analysed strides between successive right limb toe-off events (**Fig. 2**), and categorized them in accordance with two possible obstacle negotiation sequences, classified by footfall relative to the obstacle (**Fig. 3**). In one sequence, the recording limb stepped onto the obstacle directly (S 0), and the ipsilateral strides before and after obstacle contact were designated S-1 and S+1, respectively (**Fig. 3**, right leg, bottom panel, 'obstacle stride' sequence). This sequence corresponds to strides previously analysed by Daley and colleagues (Daley and Biewener, 2011). During this 'obstacle stride' sequence, the contralateral limb completes strides with stance events between S-1 and S 0 immediately before the obstacle, and between S 0 and S +1 just after the obstacle (**Fig. 3**, left leg, bottom panel, grey). We also recorded sequences in which the recording limb completes strides with stance events immediately before and after the obstacle, designated CL -1 and CL +1, with the

contralateral (non-recording) limb encountering stance on the obstacle (**Fig. 3**, top, contralateral stride sequence). In the analysis and **Fig. 3**, we have interleaved the two sequences (**Fig. 3,** middle panel) to represent the entire bilateral obstacle negotiation pattern, assuming symmetry between the right and left legs.

(a) Statistical Summary

Several linear mixed effects models were evaluated in comparison to a reference model, to test for significant effects of speed and obstacle contrast on obstacle negotiation strategy (see Methods). All models included individual as a random effect. The final model reported in **Tab. 2** is that which resulted in the lowest Akaike Information Criterion (AIC) for all measured variables (Akaike, 1976), including total muscle activity per stride (E_{tot}) and kinematic timing (see Statistical Methods). The reported model includes the fixed effects 'speed', 'strideID', and the interaction term 'speed:strideID'. The 'speed' term quantifies generic speed effects, 'strideID' quantifies the obstacle negotiation strategy (across both speeds), and 'speed:strideID' quantifies speed-specific obstacle negotiation strategy. The factor strideID has the largest explanatory power in the model (largest F-statistic, **Tab. 2**), suggesting that the overall shifts in muscle activity during obstacle negotiation are similar in magnitude between speeds. Nonetheless, across all muscles, the speed:strideID interaction term contributed significant additional explanatory power to the model (Tab. 2), based on F-statistic >1 and lower AIC compared to models without the term. The speed:strideID term reflects speed-specific differences in the stride sequence during obstacle negotiation, suggesting shifts in neuromuscular strategy. In contrast, models including the fixed effect of 'obstacle contrast', either as a main effect or an interaction term, did not improve the ANOVA model fit, as assessed by AIC. In summary, manipulating treadmill speed had a significant effect on muscle activity (E_{tot}) and kinematic timing (**Tab. 3**), whereas obstacle contrast did not. Below we report in detail the observed anticipatory and reactionary changes in hindlimb muscle activity and kinematic timing at the two treadmill speeds.

b) Anticipatory myoelectric intensity changes are larger at the slower speed

As LG activity during obstacle negotiation has been reported previously for a single speed (Daley and Biewener, 2011), we first highlight the general trends in this muscle

across terrain conditions (**Fig. 4**). During slower speed obstacle negotiation (**Fig. 4,** top), E_{tot} significantly increases intensity before the obstacle encounter, in stride CL-1. Additionally, LG shows larger fractional increases in E_{tot} strides CL-1 and S 0 when compared to the faster speed (**Fig. 4,** bottom). Within a single speed and stride category, the high and low contrast conditions (**Fig. 4,** striped *versus* plain bars) did not exhibit statistically significant differences in E_{tot}, based on Tukeys post hoc pairwise comparisons.

When changes in total muscle recruitment, E_{tot}, are examined across muscles (**Fig. 5**), the LG is representative of the overall trends. At the slower speed (**Fig. 5,** top, Tab. S1), numerous muscles show significant increases in E_{tot} during strides preceding obstacle contact, including: FPPD3 in stride S-1, and FTL, ILPO, ILPO, FPPD3, LG and MG in stride CL-1. In comparison, at the higher speed (**Fig. 5,** bottom, Tab. S2), only two muscles, FPPD3 and FCLP, show significant increase in E_{tot} preceding stride S 0. Instead, muscles exhibit larger increases in E_{tot} during the CL+1 stride, following obstacle contact, with significant increases for IF, FPPD3, LG, and MG. We did not observe statistically significant differences between low and high contrast conditions (plain versus dotted bars), based on Tukeys post hoc pairwise comparisons.

To further examine the detailed temporal changes in muscle activity during obstacle negotiation, we compared the stride-averaged myoelectric intensity trajectories between mid-flat and obstacle negotiation strides (**Fig. 6**, **Fig. 7**, and Supplemental **Fig S1 and S2** for the remaining 4 muscles**)**. In the stride preceding the obstacle (CL -1), the activity of FCLP, the multi-articular digital flexor FPPD3 and LG increased in magnitude at both speeds; however the time-course and duration of activity differs more at the lower speed (CL -1 in **Fig. 6** and **Fig. S1**). In the obstacle stride (S 0), the IF exhibits increased activity in both swing and stance phases of its double-bursting pattern, but again, changes in time-course and duration of activity are more pronounced for the slower speed (IF, in **Fig. 6**, **Fig. 7**). LG increases activity during S 0 at both speeds, but the slower speed shows a more pronounced shift in timing of peak activity toward later stance (LG, in **Fig. 6**, **Fig. 7**). Across muscles, these trajectory plots reveal larger changes in the time course of activity at the slower speed (**Fig. 6**, **Fig. S1**); whereas the characteristic shape of the activation pattern is relatively consistent at the faster speed (**Fig. 7**, **Fig. S2**). Thus, the slower speed exhibits greater

evidence of anticipatory changes in motor recruitment and stride timing during obstacle negotiation.

(b) Principal Components Analysis:

We used principal component analysis (PCA) as a quantitative tool to examine the covariance of activation changes across all measured muscles and terrain conditions. The PCA revealed that the first two principal components (PCs) explain 75% of the variance in total myoelectric intensity (E_{tot}) across all measured muscles and terrains (**Fig. S3**). The first principal component (PC1) explained 53% variance and had high positive loadings for stance antigravity and leg extensor muscles (FTL, FCLP, ILPO, FPPD3, LG, MG), and one swing-active hip flexor that contributions to limb elevation (IC). Thus, PC1 represents high-covariance among 7 of 8 measured muscles (all except IF), and might therefore correspond to limb-wide co-activation for stance antigravity support and leg shortening/lengthening. IF did exhibit substantial stride-specific shifts in activity, but did not factor strongly in PC1, possibly due to its unusual double-bursting activation pattern (**Fig. 6, Fig. 7**). The 2nd principal component (PC2) explained 22% variance and had positive loadings for muscles that assist limb retraction (FCLP, ILPO, FPPD3), and negative loadings for a hip flexor that assists limb protraction (IC), and two multi-articular muscles that cross the knee (IF, MG). These loadings suggest PC2 might correspond to leg angular excursion (protraction/retraction). Overall, the PCA results demonstrate high covariance among hindlimb muscles, suggesting synergistic activation of muscles across the limb.

Covariance along PC1 and PC2 (**Fig. 8**) reveals distinct clusters associated with stride category and speed, with high and low contrast conditions grouping together. Slow speed pre-obstacle strides CL -1 scored highest in both PC1 and PC2, whereas slow speed obstacle strides S 0 scored negatively in PC2 but positively in PC1. Positive scoring in both PC1 and PC2 (stride CL -1) is consistent with increased stance antigravity support and leg extension (+PC1) and increased leg retraction (+PC2). Positive scoring of PC1 with negative scoring in PC2 (stride S 0) is consistent with reduced limb retraction (-PC2) with increased stance antigravity support and leg extension (+PC1). The high speed, post-obstacle stride CL +1 scored moderately high in PC1, but near zero in PC2. Overall, these results suggest a greater anticipatory increase in muscle recruitment across many limb muscles at the slower speed (as

shown by higher PC scores for CL -1 at the slower speed), with comparatively lower anticipatory changes and higher reactionary changes in recruitment at the higher speed (as shown by higher PC scores for CL +1 at the faster speed).

(d) Kinematics

Consistent with muscle recruitment results, we observed larger stride-to-stride shifts in kinematic timing at the slower speed (A, **Fig. 9**) compared to the higher speed (B, **Fig. 9**). The ANOVA statistical results for kinematic timing variables reveals F-statistics > 1 for the speed:stride ID interaction term (**Tab. 3**), suggesting significant differences in obstacle negotiation strategy between the two treadmill speeds. At the slower speed, swing period increased on the obstacle (S 0) and dismounting the obstacle (CL +1), and total stride duration also increased on the obstacle (S 0). Stance duration decreased immediately following obstacle dismount (CL+1), and both stance and stride duration decreased in the subsequent post-obstacle stride (S+1). Higher contrast obstacles additionally resulted in increased stance duration preceding the obstacle (CL -1). Comparatively little stride-to-stride shifts in kinematic timing were evident during higher speed obstacle negotiation (B, **Fig. 9**), with only a significantly prolonged swing period during the obstacle dismount (CL+1) compared to mid-flat strides.

Discussion

Our findings are consistent with the idea that a treadmill locomotion environment produces context-dependent shifts in sensorimotor control, possibly due to restricted visual information. Treadmills restrict visual information by 1) reducing optical flow, because only the treadmill belt is moving, 2) reducing obstacle contrast due to uniform terrain colour and lighting, and 3) reducing available obstacle viewing time, due to its sudden appearance at the front of the belt. These factors may reduce the quality of visual information and the time available for visuomotor modulation of motor output via descending pathways. In this study, we have manipulated 1) obstacle contrast and 2) treadmill speed to investigate the sensory factors that influence use of anticipatory and reactionary neuromuscular control strategies. We hypothesize that use of anticipatory control strategies for obstacle negotiation will be greater for (1) high contrast obstacles and (2) at the slower treadmill speed.

In contrast to our expectations for hypotheses 1, obstacle contrast did not significantly influence muscle recruitment patterns during obstacle negotiation, suggesting that it is not specifically contrast perception that influences use of anticipatory strategies in this experimental context. Instead, we found that guinea fowl can use anticipatory neuromuscular control strategies to negotiate both the lower and higher contrast obstacles. However, there are some important limitations in interpreting this finding. Previous studies suggest birds are able to detect contrast with thresholds between approximately 15-30% (Ghim and Hodos 2006); however, birds exhibit substantial species-specific variation in visual function (Ghim and Hodos 2006; Martin, 2011; Martin, 2014). To our knowledge, guinea fowl visual function has not been studied in detail. If guinea fowl possess high visual acuity and contrast sensitivity, the obstacle contrast manipulation used here may not have introduced adequate perceptual change to influence anticipatory control. Even in the low contrast condition, the obstacles may have been visible due to shadowing effects. In addition, the treadmill environment may present an ecologically unnatural condition that affects how terrain is perceived, because much of the visual field is static and contradictory to the moving treadmill surface (Prokop et al., 1997). Nonetheless, our finding of significant anticipatory changes at the slower speed in both high and low contrast conditions suggest that guinea fowl do perceive sufficient visual information at both contrast conditions, at least when obstacle viewing time is sufficient.

Consistent with hypothesis 2, we observed greater anticipatory muscle modulation (preceding obstacle contact) at the slower treadmill speed. Although guinea fowl exhibited anticipatory increases in muscle activity in advance of obstacles at both speeds, these shifts are larger in magnitude (**Fig. 8**) and span more hindlimb muscles (6 versus 2, **Fig. 5**) at the slower speed. This suggests that guinea fowl increase anticipatory muscle recruitment when given more time to visually assess oncoming terrain. The results are consistent with time-dependency of anticipatory control, likely due to delays associated with visuomotor modulation via descending pathways (Patla et al., 1991). Our study provides evidence that, when timely visual sensory information is available, birds do adjust muscle recruitment in anticipation of terrain changes on a treadmill.

Interpretation of possible underlying mechanisms for observed speed effects

Considering available evidence across overground and treadmill obstacle negotiation studies, we suggest that the time available for visuomotor processing may be more critical than movement speed *per se* in determining whether birds use anticipatory strategies. When running overground, birds use anticipatory changes in leg and body dynamics to achieve steady-gait on the obstacle, even at fast running speeds (Birn-Jeffery, 2012; Birn-Jeffery and Daley, 2012; Birn-Jeffery et al., 2014). This may be because animals can adjust their gaze distance with speed to allow for visuomotor latencies when running overground. In treadmill conditions, gaze distances are restricted by the length of the treadmill. We observed more substantial anticipatory neuromuscular changes during slower speed treadmill obstacle negotiation, which provides longer obstacle viewing time. While we do observe some significant increases in muscle activity (E_{tot}) before obstacle contact at the higher speed (2 of 8 muscles, **Fig. 5**), we did not observe significant anticipatory shifts in kinematic timing **(Fig. 8)**. In contrast, overground studies find anticipatory shifts in kinematics across speeds (Birn-Jeffery, 2012; Birn-Jeffery and Daley, 2012; Birn-Jeffery et al., 2014). On the treadmill, the maximum time between obstacle appearance and its encounter was approximately 1 stride period; whereas overground, the birds could view obstacles at least 2 strides in advance (Birn-Jeffery, 2012; Birn-Jeffery and Daley, 2012; Birn-Jeffery et al., 2014). We hypothesize that obstacle viewing time (the time between the visual cue and obstacle contact) is a key factor in the ability to make visuomotor adjustments for altered terrain. However, future experiments that vary

obstacle viewing time independent of locomotor speed will be necessary to directly test this interpretation.

We also observed differences between treadmill speeds in the timing of reactionary muscle modulation (after obstacle contact), which may be related to spinal reflex feedback latencies. While short-latency spinal reflexes contribute substantially to motor output at slow and fast speeds, reflexes are highly modulated depending on task (Capaday and Stein, 1987; Ferris 1999; Stein and Capaday 1988; Zehr and Stein, 1999; Donelan et al. 2009). At slower speeds, short-latency feedback delays are small relative to stride duration (~10-25%), allowing larger within-stride feedback adjustments in response to a sensed perturbation (Reis, 1961; Cavanagh and Komi, 1979; Duysens and Loeb, 1980). At higher speeds, short-latency feedback delays can be greater than 50% of stance duration, which can make reflexes destabilising (Kuo, 2002). This may explain why short-latency reflex responses tend to be down-regulated at higher speeds (Capaday and Stein, 1987; Ferris 1999). Comparing the two speed conditions in the current study, the slower speed showed comparatively higher positive scores for PC1 on the obstacle step (S 0, **Fig. 8**). In contrast, the faster speed showed higher positive scores for PC1 in the obstacle dismount stride (CL +1, **Fig. 8**). Thus the slower speed showed greater within-stride modulation of activity upon obstacle contact, whereas the higher speed relied more heavily on recovery upon dismount from the obstacle. These findings are consistent with greater reliance on longer-latency responses at higher speeds, similar to previous studies (da Silva et al., 2011).

Our findings are also consistent with a shift in intrinsic mechanical stability between speed conditions. We define *intrinsic stability mechanisms* as those that arise from the natural dynamics of the mechanical system due to inertia, momentum and mechanical energy of the body and limbs (Jindrich and Full, 2002; Moritz and Farley, 2004; Matthis and Fajen, 2013). Despite substantial and widespread shifts in muscle recruitment during obstacle negotiation at both speeds, we observe little change in kinematic timing at the higher speed (**Fig. 9**, bottom), with a significant change only in the swing duration of the obstacle dismount stride (CL +1). In contrast, the slower speed showed significant shifts in kinematic timing in strides before, during and following obstacle contact (**Fig. 9**, top). The mechanical effects of altered recruitment may be restricted at higher speed due to the combined effects of neuromechanical

delays and increased intrinsic stability. Intrinsic mechanical stability can be beneficial in bridging unavoidable neural control gaps (Daley et al., 2009; John et al., 2013). However, such mechanical effects are necessarily bi-directional—while intrinsic stability reduces sensitivity to external perturbations, it also reduces responsiveness to changes in muscle activity. Previous studies in cockroaches found that the effects of a specific increase in muscle activation on body dynamics depend strongly on dynamic context (Sponberg et al., 2011a; Sponberg et al., 2011b). Thus, at different speeds, similar increases in EMG activity may not result in similar mechanical effects. In the current results, the absence of kinematic shifts at the higher speeds, even in strides with significantly increased muscle activity (e.g., strides CL-1 and S0, **Fig. 5** and **Fig. 9**), suggests greater intrinsic stability at the higher speed.

Changing treadmill speed induces other integrated speed effects, including a shift in stance duration, duty factor, peak forces and gait dynamics. Avian bipeds exhibit a gradual transition between walking and running, including 'grounded running' at intermediate speeds (Gatesy, 1991; Gatesy 99a). This makes it difficult to clearly distinguish between gaits without ground reaction forces and detailed body dynamics, which we do not have here. Nonetheless, higher speed does require larger peak forces and higher muscle activation to support body weight. To focus our analysis specifically on obstacle negotiation strategy, we normalized E_{tot} relative to the level terrain mean at the same speed, so that pair-wise comparisons between stride categories reflected shifts during obstacle negotiation, not shifts associated with speed alone. Additionally, we used statistical models that included speed as an independent factor and a 'speed:strideID' interaction term, which allowed quantification of generic speed effects separate from speed-specific obstacle negotiation strategy (see Results: Statistical Summary). Further, the PCA results revealed similar co-variance patterns among hindlimb muscles between speeds. These findings suggest similar overall neuromuscular control for locomotion between speeds, despite some shifts in use of anticipatory, reactionary and intrinsic stability mechanisms, discussed above.

Implications for neuromechanical control models of bipedal locomotion

Previous work has suggested a proximo-distal gradient in limb neuromuscular function, in which distal limb muscles exhibit greater reactionary modulation due to reflex feedback and intrinsic mechanical sensitivity (Daley et al., 2007). In the current

study, however, we did not find evidence for a proximo-distal gradient. This is particularly evident from the principle component analysis (PCA), in which we found that recruitment co-varied strongly across many hindlimb muscles (**Fig. 8**), without a proximo-distal distinction.

Why the absence of a proximo-distal gradient, despite its previous observation at the level of limb joint mechanics? In the current study, both anticipatory, feedforward changes and feedback-mediated changes are likely to have contributed to the observed changes in recruitment. In contrast, the previous study focused on the 'reactive' response to an unexpected perturbation (Daley et al., 2007) and not an anticipated manoeuvre. The observed proximo-distal gradient is likely to have resulted from a combination of intrinsic mechanical factors and feedback-mediated changes, without anticipatory effects. Here, we did observe slightly higher magnitude shifts in EMG activity in the distal compared to proximal muscles in the obstacle dismount stride (**Fig. 5**, CL+1), consistent with higher gain load-dependent feedback in the distal muscles, as suggested in a previous cat study (Nichols and Ross, 2009). However, an important limitation of the current and previous guinea fowl studies is the lack of simultaneous measurements of joint dynamics and hindlimb muscle activity, as the current study focuses on muscle activity, whereas the previous focused on joint dynamics (Daley et al., 2007). The link between muscle activation and joint dynamics is indirect, depending on the physical properties of the limb segments and the action of multi-articular muscles in transmitting force and energy between joints (Prilutsky, 2000). It therefore remains to be investigated whether the limb-wide co-variation in muscle recruitment observed here maps to comparable limb-wide changes in joint dynamics.

Nonetheless, the PCA results here do reveal synergistic co-activation of muscles across the limb, rather than independent control of individual muscles. This finding suggests that a relatively simple reduced-order control model might be able to reproduce the observed limb-wide co-variation in muscle activity, consistent with the idea that control is simplified through muscle synergies arising from spinal neural networks (d'Avella and Bizzi; Chvatal and Ting 2012; Bizzi and Cheung 2013). For example, control commands might relate to limb extension and limb retraction, representing a reduced-order model of bipedal locomotion similar to those presented

in Birn-Jeffery et al. (2014) and Van why et al. (2014). In future work, it will be interesting to investigate the specific mapping between detailed musculoskeletal dynamics and reduced-order neuromechanical control 'templates' (*sensu* Full 1999) for bipedal locomotion.

Conclusions

Guinea fowl make greater use of anticipatory control strategies during slower speed treadmill obstacle negotiation, as compared to higher speed, demonstrating context-dependent neuromuscular control. We suggest that this finding relates to greater time available for visuomotor processing at slower speeds on a treadmill, due to higher available obstacle viewing time. When taken in context of previous literature, our results suggest that a treadmill environment may enhance speed-dependent differences in sensorimotor control, possibly due to both sensory and mechanical effects, including restricted visual information, restricted manoeuvring space on the treadmill belt, and speed-related changes in intrinsic mechanical stability.

Methods

(a) Animals and training

We obtained six adult guinea fowl (*Numida meleagris*) with 1.6kg ± 0.23 kg body mass from Devon, UK. We trained birds to run on a level motorized treadmill (Woodway, Waukesha, WI, USA) at speeds up to 2ms^{-1}, with training sessions of 15-20 minutes in duration, with breaks for 2 minutes as needed. Each bird received 3-4 days training per week for three weeks before our study commenced. We undertook all experiments at the RVC Structure and Motion Laboratory with all animal procedures licensed and approved by the UK Home Office.

(b) Surgical Procedures

Birds received a premedication of 0.2mgkg^{-1} intramuscular Butorphanol 15 minutes prior to induction. Sevofluorane was used to induce anaesthesia through a mask followed by intubation with a non-cuffed endotracheal tube and continued gaseous maintenance of mid-plane anaesthesia throughout the remainder of the procedure. Perioperative antibiotics and anti-inflammatories were administered intramuscularly

after induction. Three skin incisions of 3-5cm were made over the right caudal thigh, cranial thigh and lateral shank to enable direct visualisation and intramuscular electrode placement in 8 superficially accessible muscles distributed proximal and distal to the knee (**Fig. 1**). Electrodes had been previously constructed from two strands of 38 gauge teflon-coated stainless steel (AS 632, Cooner Wire Co., California, USA) with staggered 1mm exposed wire region spaced 1.5mm apart. Both electrodes were placed simultaneously using sew-through methods and silicon anchors (3 x 3 x 2mm) positioned with a single square knot at the muscle surface-electrode interface (Deban and Carrier, 2002). Wires were tunnelled together subcutaneously through silicon tubing using a looped guide wire through a 1.5cm incision made over the dorsal synsacrum. Leg incisions were then closed with 2 metric nylon sutures. The dorsal incision was closed using a purse-string nylon 2 metric suture around the silicon tubing before a nylon finger-trap was secured. All electrodes were then soldered into a D-type multi-pin connector. Excess wiring was re-introduced into the silicon tubing and quick drying adhesive (Araldite$_{TM}$ Rapid) used to create a protective insulated seal encompassing the tube end and newly soldered connections. All birds recovered to standing within 30 minutes of surgery. Carprofen was administered at 1mgkg^{-1} once daily and Enrofloxacin 10mgkg^{-1} twice daily during the experimental period. After the data collection was complete, a second anaesthesia was performed as above to enable electrode inspection, verification and removal. All birds recovered and healed post surgery.

(c) EMG Recordings

The micro-connector on the dorsal synsacrum was connected via a purpose-built lightweight shielded cable to 8 GRASS differential voltage amplifiers. EMG signals remained at a constant amplification throughout data collection with low (10Hz) and high (3kHz) pass filtering. EMG signals were sampled using an A/D converter at 4920 Hz using a customized Labview program interface (National Instruments Corporation Ltd., UK).

(d) **Kinematics**

Digital high speed video was recorded in lateral view at 120Hz (AOS High Resolution). Major joints were highlighted using high contrast adhesive markers.

(e) **Experimental protocol**

The guinea fowl were run for 30-second trials spaced with 10 minutes rest periods during which the birds were given access to food and water. Three trials were recorded for each condition over a two-day period. We recorded data at two speeds ($0.7ms^{-1}$, Froude 0.25 and $1.3ms^{-1}$, Froude 0.86) and three terrain conditions at each speed: (i) level, (ii) repeated 5cm low contrast obstacles (black), and (iii) repeated 5cm high contrast obstacles (black with white stripes). We selected the specific speeds to provide a substantial difference in the obstacle viewing time, while remaining within the range of speeds the birds could comfortably maintain on the treadmill. The treadmill belt was slatted black rubber-coated steel with running surface 55.8cm x 172.7cm with sufficient clearance to allow free passage of obstacles beneath the treadmill. Obstacles were constructed from a balsa wood base covered with black neoprene, and high contrast was introduced using white felt stripes. Heavy-duty hook and loop fastener was used to attach the obstacles to the treadmill surface. Four obstacles were placed on sequential slats creating a $20cm^2$ obstacle surface be negotiated once per belt rotation. Birds encounter obstacles every 4-5 strides at the faster speed, and 5-6 strides at the slower speed (due to shorter stride lengths at the slower speed).

We designed the high and low contrast obstacles to maximize the difference in contrast signal between conditions. Birds have lower contrast sensitivity than mammals; however, they are able to detect contrast with thresholds between approximately 15-30%, depending on species and the spatial frequency of presented contrast signal (Ghim and Hodos 2006). The obstacles in this study subtended a relatively large visual angle while moving backwards on the treadmill belt, facilitating contrast detection (Ghim and Hodos 2006). The 'low contrast' obstacles exhibited <10% contrast from the belt (black/black), and the 'high contrast' obstacles exhibited >90% contrast (black/white). Thus, the low contrast obstacles were near the undetectable range for birds, whereas the high contrast obstacles were safely within the detectable range, assuming that guinea fowl have contrast sensitivity comparable to other birds.

 (f) **Data Processing**

Videos were observed and frame times manually recorded for right foot stride sequences using Virtual Dub software. Strides were identified based on their sequence in relation to obstacle contact, and as only single-limb instrumentation was undertaken, two possible alternate obstacle negotiation sequences were separately analysed (**Fig. 3**). A sequentially ordered sequence of strides IDs was re-constructed from these two sequences, representing the full bilateral obstacle negotiation sequence, assuming symmetry between right and left legs. These stride IDs were coded as a fixed effect factor for further analysis and statistics.

Raw EMG signals were used to calculate the myoelectric intensity of the EMG signal in time-frequency space using wavelet decomposition (von Tscharner, 2000; Wakeling et al., 2002). We used a bank of 16 wavelets with time and frequency resolution optimized for muscle, with wavelet centre frequencies ranging from 6.9 to 804.2Hz (von Tscharner, 2000). The intensity over wavelets 92.4 to 804.2 Hz at each time-point was then summed to calculate the instantaneous myoelectric intensity (mV^2). This provides a smooth trace of EMG intensity over time that accounts for the entire physiological frequency range and acts to exclude noise from the calculation. Instantaneous intensity traces (mV^2) were cut into strides and categorized by stride, normalized by the mean peak intensity of level terrain strides, for each specific muscle and bird at the same speed. Total myoelectric intensity per stride was calculated by integrating this intensity wave over time (mV^2s) for each stride interval. The resulting total intensities (E_{tot}) were normalized by the level terrain mean at the same speed, prior to further statistical analysis. Such normalization ensured that shifts in E_{tot} during obstacle negotiation reflected differences relative to level terrain at the same speed, to minimize effects due to speed alone. Data processing was completed using MATLAB (Mathworks, Inc.; Natick, MA, USA).

(g) **Statistics**

A linear-mixed effects model was used to test for significant effects of speed, contrast (obstacle contrast) and stride ID (obstacle negotiation strategy), on the dependent variables E_{tot} for each muscle, stride duration, stance duration and swing duration (**Tab. 2 & 5**). Several linear mixed effects models were evaluated in comparison to a reference model, as detailed below. The final model reported is that which resulted in

the lowest Akaike Information Criterion (AIC) for all dependent factors, calculated as AIC = 2K - 2log(L) (Akaike, 1976), where k is the number of predictors in the model, and L is the maximum likelihood value. The AIC provides a method of comparing the goodness of fit of multiple models, and penalizes for the number of parameters in the model, promoting parsimonious model selection. The model with lowest AIC is preferred. Fixed effects included in model comparison were speed, stride ID, speed:stride ID (to test for effect of obstacle viewing time on obstacle negotiation strategy), contrast and contrast:stride ID (to test for the effect of contrast on obstacle negotiation strategy). All models included individual (bird ID) as a random effect to account for individual variation. The LME and post-hoc pairwise comparison Tukey's tests were applied using the open source R software (lme4 and multcomp packages).

Several specific models were evaluated in comparison to a reference model to test the proposed hypotheses and ensure that variance in data was characterized using the simplest possible model. Reference and alternative models were compared, as below, for all dependent factors ('factor'= one of the dependent factors, either : E_{tot}, stride duration, swing duration, stance duration). The reference model includes the independent factors of speed and strideID, plus the random effect of individual. This model represents the null hypotheses that 1) there is no significant effect of speed on obstacle negotiation strategy (omitting the speed:stride ID term), and 2) there is no significant effect of contrast on obstacle negotiation strategy (omitting the contrast:stride ID term).

Reference model: factor ~ speed + strideID + bird ID

Alternative models:

1. factor ~ speed + stride ID + speed:stride ID + bird ID
2. factor ~ speed + stride ID + contrast + bird ID
3. factor ~ speed + stride ID + contrast:stride ID + bird ID
4. factor ~ speed + stride ID + contrast + contrast:stride ID + bird ID

The model reported, with the lowest AIC for each factor, was:

 factor ~ speed + stride ID + speed:stride ID + bird ID

We used tukeys post hoc pairwise comparisons to further explore the specific changes in obstacle negotiation, comparing each obstacle negotiation stride to reference mid-flat strides in low contrast terrain, within each speed (significance value set at $p \leq 0.05$). We additionally graphically compare the averaged activation trajectories between mid-flat and obstacle negotiation strides, to observe qualitative changes through time.

A principal components analysis (PCA) was performed in MATLAB (Mathworks, Inc.; Natick, MA, USA) to analyse covariance patterns in E_{tot} across all 8 measured hindlimb muscles, with the PCA dataset including the grand mean E_{tot} for each muscle and each stride category across both speeds and all three terrains (level, high contrast obstacles, low contrast obstacles).

List of Symbols/Abbreviations

AIC	-	akaike information criterion
E_{tot}	-	total myoelectric intensity
EMG	-	electromyography
Stride ID	-	stride identity
Bird ID	-	individual identity
PC1	-	principal component 1
PC2	-	principal component 2
PCA	-	principal component analysis
IC	-	iliotibialis cranialis
IF	-	iliofibularis lateralis
FTL	-	femorotibialis lateralis
ILPO	-	iliotibialis lateralis postacetabularis
LG	-	lateral gastrocnemius
MG	-	medial gastrocnemius
FPPD3	-	flexores perforati digiti III
FCLP	-	flexor cruris lateralis pelvica
SEM	-	standard error of the mean

References

Akaike, H. (1976). An information criterion (AIC). *Math Sci 14* **153**, 5-9.

Belmonti, V., Cioni, G. and Berthoz, A. (2013). Development of anticipatory orienting strategies and trajectory formation in goal-oriented locomotion. *Exp Brain Res* **227**, 131-147.

Birn-Jeffery, A. V. (2012). Scaling of running stability and limb posture with body size in galliform birds. *PhD Thesis* Royal Veterinary College, UK.

Birn-Jeffery, A. V. and Daley, M. A. (2012). Birds achieve high robustness in uneven terrain through active control of landing conditions. *J Exp Biol* **215**, 2117-2127.

Birn-Jeffery, A. V., Hubicki, C. M., Blum, Y., Renjewski, D., Hurst, J. W. and Daley, M. A. (2014). Don't break a leg: running birds from quail to ostrich prioritise leg safety and economy on uneven terrain. *J Exp Biol* **217**, 3786-3796.

Bizzi, E., and Cheung, V. C. (2013). The neural origin of muscle synergies. *Front Comput Neurosci* **7**, 51.

Blum, Y., Vejdani, H. R., Birn-Jeffery, A. V., Hubicki, C. M., Hurst, J. W. and Daley, M. A. (2014). Swing-leg trajectory of running guinea fowl suggests task-level priority of force regulation rather than disturbance rejection. *PloS one* **9**, e100399.

d'Avella, A., and Bizzi, E. (2005). Shared and specific muscle synergies in natural motor behaviors. *Proc Natl Acad Sci USA* **102**, 3076-3081.

Capaday, C. and Stein, R. B. (1987). Difference in the amplitude of the human soleus H reflex during walking and running. *J Physiol* **392**, 513-522.

Cavanagh, P. R. and Komi, P. V. (1979). Electromechanical delay in human skeletal muscle under concentric and eccentric contractions. *Eur J Appl Physiol Occup Physiol* **42**, 159-163.

Chvatal, S. A., and Ting, L. H. (2012) Voluntary and reactive recruitment of locomotor muscle synergies during perturbed walking. *J Neurosci* **32,** 12237-12250.

Cinelli, M. E. and Patla, A. E. (2008). Task-specific modulations of locomotor action parameters based on on-line visual information during collision avoidance with moving objects. *Hum Mov Sci* **27**, 513-531.

da Silva, J. J., Barbieri, F. A. and Gobbi, L. T. (2011). Adaptive locomotion for crossing a moving obstacle. *Motor control* **15**, 419-433.

Daley, M. A. and Biewener, A. A. (2011). Leg muscles that mediate stability: mechanics and control of two distal extensor muscles during obstacle negotiation in the guinea fowl. *Phil Trans Royal Society B* **366**, 1580-1591.

Daley, M. A., Felix, G. and Biewener, A. A. (2007). Running stability is enhanced by a proximo-distal gradient in joint neuromechanical control. *J Exp Biol* **210**, 732-732.

Daley, M. A., Voloshina, A. and Biewener, A. A. (2009). The role of intrinsic muscle mechanics in the neuromuscular control of stable running in the guinea fowl. *J Physiol* **587**, 2693-2707.

Deban, S. M. and Carrier, D. R. (2002). Hypaxial muscle activity during running and breathing in dogs. *J Exp Biol* **205**, 1953-1967.

Dickinson, M. H., Farley, C. T., Full, R. J., Koehl, M. A., Kram, R. and Lehman, S. (2000). How animals move: an integrative view. *Science* **288**, 100-106.

Donelan, J. M., McVea, D. A. and Pearson, K. G. (2009). Force regulation of ankle extensor muscle activity in freely walking cats. *J Neurophysiol* **101**, 360-371.

Duysens, J. and Loeb, G. E. (1980). Modulation of ipsilateral and contralateral reflex responses in unrestrained walking cats. *J Neurophysiol* **44**, 1024-1037.

Fajen, B. R., Parade, M. S. and Matthis, J. S. (2013). Humans perceive object motion in world coordinates during obstacle avoidance. *J Vis* **13**, 8, 25.

Fowler, G. A. and Sherk, H. (2003). Gaze during visually-guided locomotion in cats. *Behav Brain Res* **139**, 83-96.

Frigon, A. and Rossignol, S. (2006). Experiments and models of sensorimotor interactions during locomotion. *Biol Cybern* **95**, 607-627.

Full, R. J., and Koditschek, D. E. (1999). Templates and anchors: neuromechanical hypotheses of legged locomotion on land. *J Exp Biol* **202**, 3325-3332.

Gatesy, S. M. B., A. A. . (1991). Bipedal locomotion: effects of speed, size and limb posture in birds and humans. *J Zool* **Volume 224**, 127-147.

Ghez, C. and Vicario, D. (1978). The control of rapid limb movement in the cat. I. Response latency. *Exp Brain Res* **33**, 173-189.

Ghim, M. M., & Hodos, W. (2006). Spatial contrast sensitivity of birds. *J Comp Physiol A* **192**, 523-534.

Hollands, M. A., Patla, A. E. and Vickers, J. N. (2002). "Look where you're going!": gaze behaviour associated with maintaining and changing the direction of locomotion. *Exp Brain Res* **143**, 221-230.

Jindrich, D. L. and Full, R. J. (2002). Dynamic stabilization of rapid hexapedal locomotion. *J Exp Biol* **205**, 2803-2823.

John, C. T., Anderson, F. C., Higginson, J. S. and Delp, S. L. (2013). Stabilisation of walking by intrinsic muscle properties revealed in a three-dimensional muscle-driven simulation. *Comput Methods Biomech Biomed Engin* **16**, 451-462.

Kuo, A. D. (2002). The relative roles of feedforward and feedback in the control of rhythmic movements. *Motor control* **6**, 129-145.

Marigold, D. S. and Patla, A. E. (2007). Gaze fixation patterns for negotiating complex ground terrain. *Neuroscience* **144**, 302-313.

Marigold, D. S. and Patla, A. E. (2008). Visual information from the lower visual field is important for walking across multi-surface terrain. *Exp Brain Res* **188**, 23-31.

Martin, G. R. (2011). Understanding bird collisions with man-made objects: a sensory ecology approach. *Ibis* **153**, 239-254.

Martin, G. R. (2014). The subtlety of simple eyes: the tuning of visual fields to perceptual challenges in birds. *Phil Trans Royal Society B* **369**, 20130040.

Matthis, J. S. and Fajen, B. R. (2013). Humans exploit the biomechanics of bipedal gait during visually guided walking over complex terrain. *Proc Biol Sci* **280**, 20130700.

Matthis, J. S. and Fajen, B. R. (2014). Visual control of foot placement when walking over complex terrain. *J Exp Psychol Hum Percept Perform* **40**, 106-115.

Mohagheghi, A. A., Moraes, R. and Patla, A. E. (2004). The effects of distant and on-line visual information on the control of approach phase and step over an obstacle during locomotion. *Exp Brain Res* **155**, 459-468.

Moritz, C. T. and Farley, C. T. (2004). Passive dynamics change leg mechanics for an unexpected surface during human hopping. *J Appl Physiol* **97**, 1313-1322.

Moritz, C. T. and Farley, C. T. (2005). Human hopping on very soft elastic surfaces: implications for muscle pre-stretch and elastic energy storage in locomotion. *J Exp Biol* **208**, 939-949.

Muller, R., Grimmer, S. and Blickhan, R. (2010). Running on uneven ground: leg adjustments by muscle pre-activation control. *Hum Mov Sci* **29**, 299-310.

Nichols, R. and Ross, K. T. (2009). The implications of force feedback for the λ model. In *Progress in Motor Control*, pp. 663-679: Springer.

Nishikawa, K., Biewener, A. A., Aerts, P., Ahn, A. N., Chiel, H. J., Daley, M. A., Daniel, T. L., Full, R. J., Hale, M. E., Hedrick, T. L. et al. (2007). Neuromechanics: an integrative approach for understanding motor control. *Integr Comp Biol* **47**, 16-54.

Patla, A. E. (1997). Understanding the roles of vision in the control of human locomotion. *Gait & Posture* **5**, 54-69.

Patla, A. E. (1998). How Is Human Gait Controlled by Vision. *Ecological Psychology* **10**, 287-302.

Patla, A. E. and Vickers, J. N. (2003). How far ahead do we look when required to step on specific locations in the travel path during locomotion? *Exp Brain Res* **148**, 133-138.

Patla, A. E., Prentice, S. D., Robinson, C. and Neufeld, J. (1991). Visual control of locomotion: strategies for changing direction and for going over obstacles. *J Exp Psychol Hum Percept Perform* **17**, 603-634.

Patla, A. E., Niechwiej, E., Racco, V. and Goodale, M. A. (2002). Understanding the contribution of binocular vision to the control of adaptive locomotion. *Exp Brain Res* **142**, 551-561.

Pearson, K. (2000). Motor systems. *Curr Opin Neurobiol* **10**, 649-654.

Prilutsky, B. I. (2000). Coordination of two- and one-joint muscles: functional consequences and implications for motor control. *Motor control* **4**, 1-44.

Prochazka, A. and Ellaway, P. (2012). Sensory systems in the control of movement. *Compr Physiol* **2**, 2615-2627.

Prokop, T., Schubert, M. and Berger, W. (1997). Visual influence on human locomotion. Modulation to changes in optic flow. *Exp Brain Res* **114**, 63-70.

R_Development_Core_Team. (2008). R: A language and environment for statistical computing. R Foundation for Statistical Computing, Vienna, Austria.

Reis, D. J. (1961). The palmomental reflex. A fragment of a general nociceptive skin reflex: a physiological study in normal man. *Arch Neurol* **4**, 486-498.

Rietdyk, S. and Drifmeyer, J. E. (2010). The rough-terrain problem: accurate foot targeting as a function of visual information regarding target location. *J Mot Behav* **42**, 37-48.

Ross, K. T. and Nichols, T. R. (2009). Heterogenic feedback between hindlimb extensors in the spontaneously locomoting premammillary cat. *J Neurophysiol* **101**, 184-197.

Sponberg, S., Libby, T., Mullens, C. H. and Full, R. J. (2011a). Shifts in a single muscle's control potential of body dynamics are determined by mechanical feedback. *Phil Trans Royal Society* **366**, 1606-1620.

Sponberg, S., Spence, A. J., Mullens, C. H. and Full, R. J. (2011b). A single muscle's multifunctional control potential of body dynamics for postural control and running. *Phil Trans Royal Society* **366**, 1592-1605.

Van Why, J., Hubicki, C., Jones, M., Daley, M., & Hurst, J. (2014). Running into a trap: Numerical design of task-optimal preflex behaviors for delayed disturbance responses. *IROS (IEEE/RSJ International Conference),* 2537-2542.

Voloshina, A. S., Kuo, A. D., Daley, M. A. and Ferris, D. P. (2013). Biomechanics and energetics of walking on uneven terrain. *J Exp Biol* **216**, 3963-3970.

von Tscharner, V. (2000). Intensity analysis in time-frequency space of surface myoelectric signals by wavelets of specified resolution. *J Electromyogr Kinesiol* **10**, 433-445.

Wakeling, J. M., Kaya, M., Temple, G. K., Johnston, I. A. and Herzog, W. (2002). Determining patterns of motor recruitment during locomotion. *J Exp Biol* **205**, 359-369.

Weerdesteyn, V., Nienhuis, B., Hampsink, B. and Duysens, J. (2004). Gait adjustments in response to an obstacle are faster than voluntary reactions. *Hum Mov Sci* **23**, 351-363.

Yakovenko, S., Gritsenko, V. and Prochazka, A. (2004). Contribution of stretch reflexes to locomotor control: a modeling study. *Biol Cybern* **90**, 146-155.

Yakovenko, S., McCrea, D. A., Stecina, K. and Prochazka, A. (2005). Control of locomotor cycle durations. *J Neurophysiol* **94**, 1057-1065.

Zehr, E. P. and Stein, R. B. (1999). What functions do reflexes serve during human locomotion? *Prog Neurobiol* **58**, 185-205.

Tables

Table 1. Summary of typical activity pattern proposed function of the eight measured hindlimb muscles (Adapted from Gatesy 1999). Abbreviations as in **Fig. 1**.

Muscle	Phase of activity	Burst timing	Action
IC	swing	late stance to late swing	hip flexor knee extensor
FTL	stance	late swing to late stance	mono-articular knee extensor
ILPO	stance	late swing to early stance	hip extensor knee extensor (possible hip abductor)
FCLP	stance	late swing to late stance	hip extensor knee flexor (possible hip abductor)
IF	swing and stance	biphasic, swing and stance bursts	hip extensor knee flexor
FPPD3	stance	late swing to late stance	ankle extensor digital flexor
LG	stance	late swing to late stance	ankle extensor knee flexor
MG	stance	late swing to late stance	ankle extensor knee flexor

Table 2. Summary of linear mixed effects model results for effects of speed, stride ID and their interaction on total myoelectric intensity (E_{tot}), for all muscles recorded. Bird ID was included as a random factor in all models. Degrees of freedom for each factor are: speed = 1, stride ID = 5, speed:stride ID = 5

Total EMG stride intensity (E_{tot})	F stat			AIC
	speed	stride ID	speed:stride ID	
IC	3.1	55.5	6.0	1631
FTL	9.6	39.7	14.6	1627
FCLP	14.8	37.9	7.4	2648
IF	16.8	35.8	7.8	1941
ILPO	17.4	55.0	6.4	2336
FPPD3	2.6	156.3	21.3	2334
LG	9.8	102.2	19.4	3822
MG	0.4	44.0	6.3	2900

Table 3. Summary of linear mixed effects model results for effects of speed, stride ID and their interaction on kinematic timing variables. Bird ID was included as a random factor in all models. Degrees of freedom for each factor are: speed = 1, stride ID = 5, speed:stride ID = 5. Statistically significant Tukey's posthoc pairwise comparisons (p ≤ 0.05) between obstacle strides and mid flat strides are indicated by asterisks in **Fig. 9**.

Kinematic factor	F stat			AIC
	speed	stride ID	speed:stride ID	
swing duration	624.8	120.6	78.7	-10598
stance duration	5487.2	47.1	24.2	-7493.6
stride duration	6492.1	33.1	37.8	-7167.5

Figures

Legend:
- M. iliotibilialis cranialis (IC)
- M. femorotibialis lateralis (FTL)
- M. flexor cruris lateralis pelvica (FCLP)
- M. iliofibularis lateralis (IF)
- M. iliotibialis lateralis postacetabularis (ILPO)
- M. flexores perforati digiti III (FPPD3)
- M. gastrocnemius pars lateralis (LG)
- M. gastrocnemius pars medialis (MG)
- • EMG Electrode Position
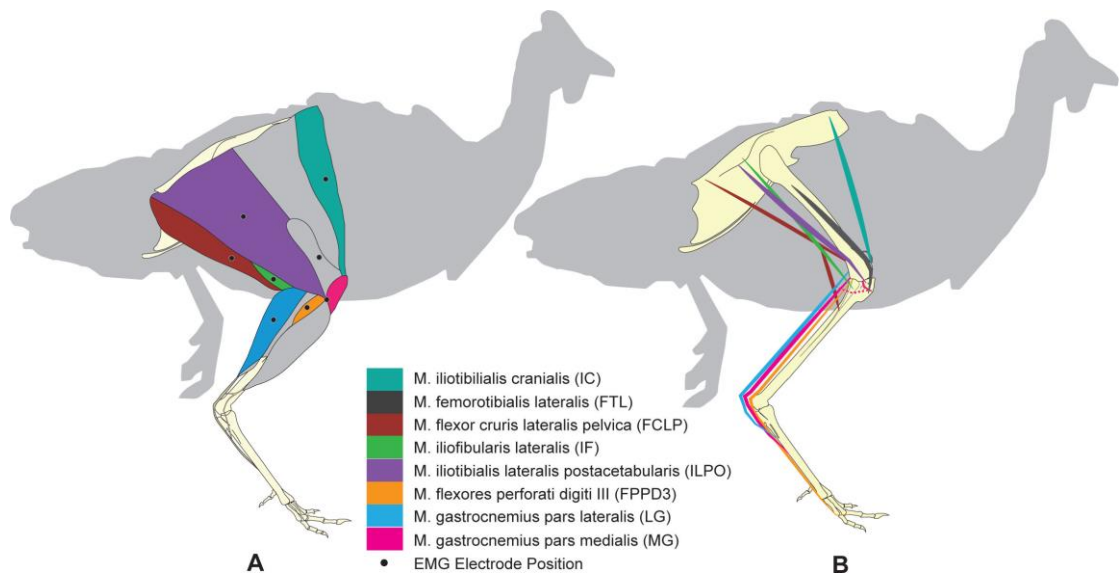
Figure 1. Schematic of guinea fowl hindlimb anatomy and EMG electrode placement. A) Schematic muscle anatomy and placement of the 8 electrodes. B) Schematic skeletal anatomy with each muscle's line of action to illustrate origin and insertion. Dashed line represents medial section of the proximal head of the MG.
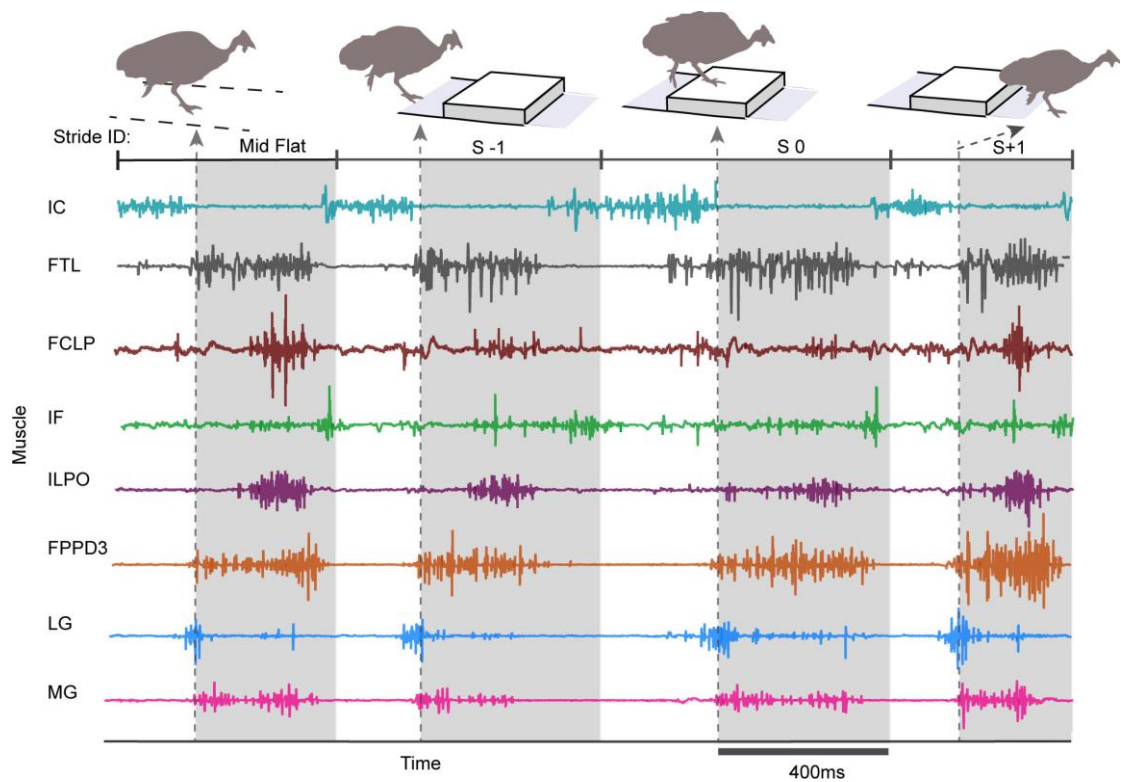
Figure 2. A representative four-stride sequence of raw EMG data recorded from eight guinea fowl hindlimb muscles during treadmill obstacle negotiation in the high contrast, slower speed condition. Grey shaded regions indicate stance phase of the instrumented limb. Data are shown for one of two possible stride sequences (see **Fig. 3**) as the bird approaches, steps onto and over the obstacle. The recording limb underwent stance phase on top of the obstacle in stride ID 'S 0'
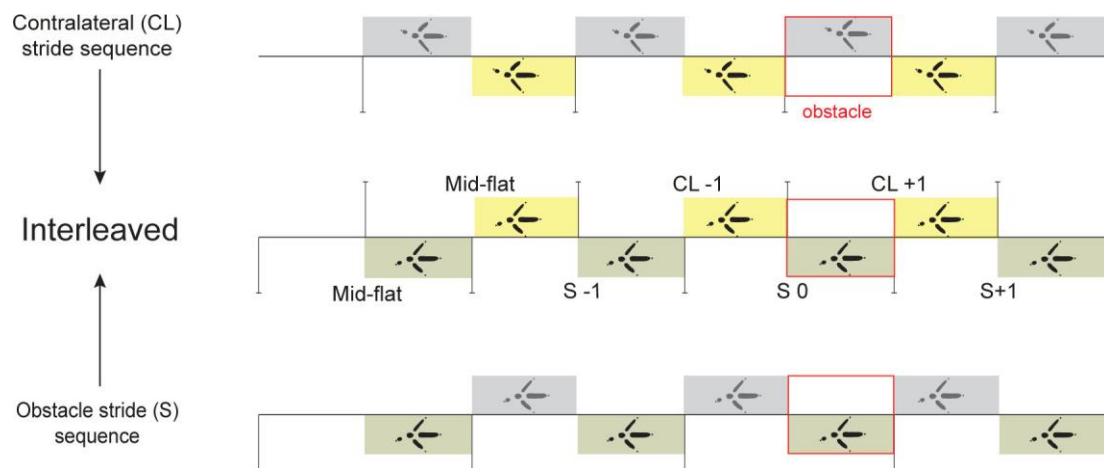
Figure 3. Schematic representation of the two possible stride sequences of the instrumented right limb during obstacle negotiation, depicted from an 'overhead' foot step view. Data cutting points are indicated by vertical black lines. The obstacle footfall event is outlined in red. The bottom panel depicts the obstacle stride footfall sequence ('S'), in which the instrumented right leg enters a stance phase on the obstacle (S 0), and the non-recording left leg undergoes stance directly before and after the obstacle. The top panel depicts the alternate contralateral footfall stride sequence ('CL'), in which the instrumented right leg undergoes stance directly before (CL -1) and after (CL +1) the obstacle, whereas the non-recording leg enters stance on the obstacle. The middle panel shows these stride sequences interleaved, where instrumented limb data are used to produce a complete bilateral obstacle negotiation sequence, assuming symmetry between right and left legs. Stride IDs shown in the middle panel are used in subsequent figures.
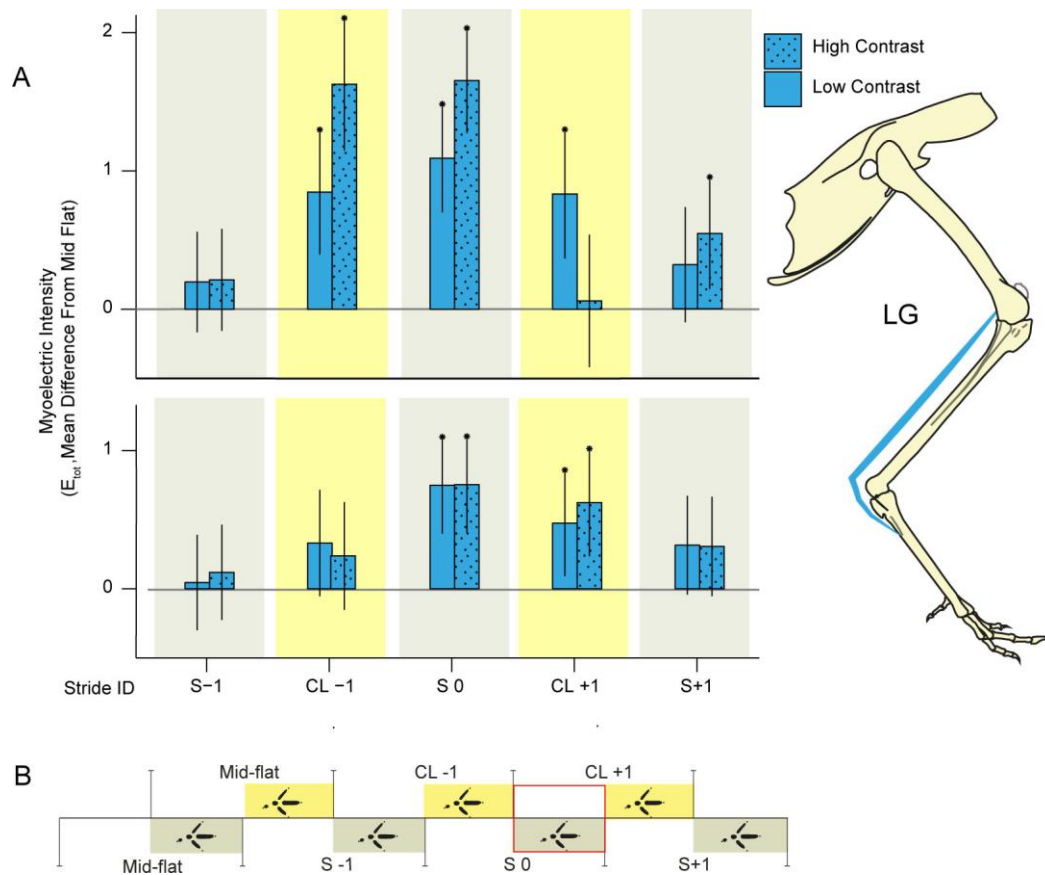
Figure 4. Changes in total myoelectric intensity per stride (E_{tot}) during obstacle negotiation in the lateral gastrocnemius (LG), as a fractional difference from mid-flat strides. A) Changes in LG E_{tot} at the slower speed (top) and higher speed (bottom), for the bilateral obstacle negotiation sequence (B, **Fig. 3**). Low and high contrast obstacle conditions are shown with solid and dotted bars, respectively. Bars indicate grand mean differences from mid-flat strides, with error bars indicating standard error for the mean (s.e.m.) and asterisks for statistically significant posthoc pairwise differences from mid-flat strides ($p \leq 0.05$).
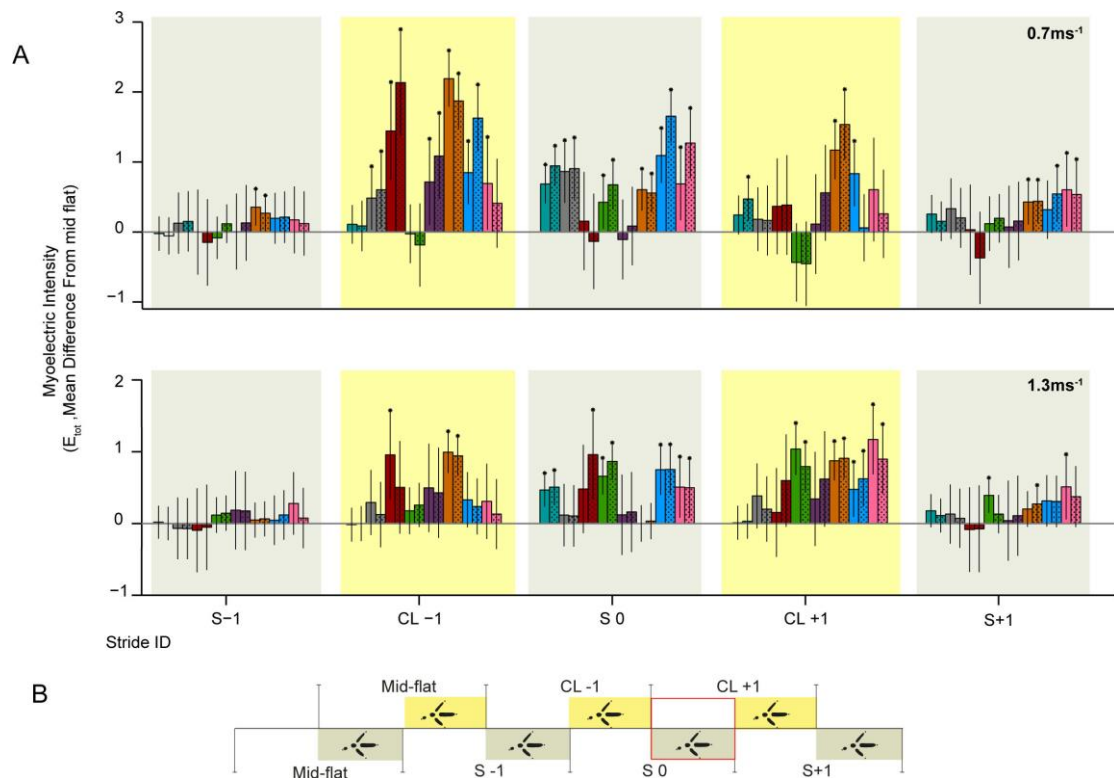
Figure 5. Changes in E_{tot} during obstacle negotiation as a fractional difference from mid-flat strides, for all 8 recorded hindlimb muscles. Colour legend as in **Fig. 1**, with solid and dotted bars indicating low and high contrast obstacle conditions, respectively. Bars indicate grand mean differences in E_{tot} from mid-flat strides during the bilateral obstacle negotiation sequence (B, **Fig. 3**). Error bars indicate s.e.m. and asterisks show statistically significant posthoc pairwise differences from mid flat strides ($p \leq 0.05$).
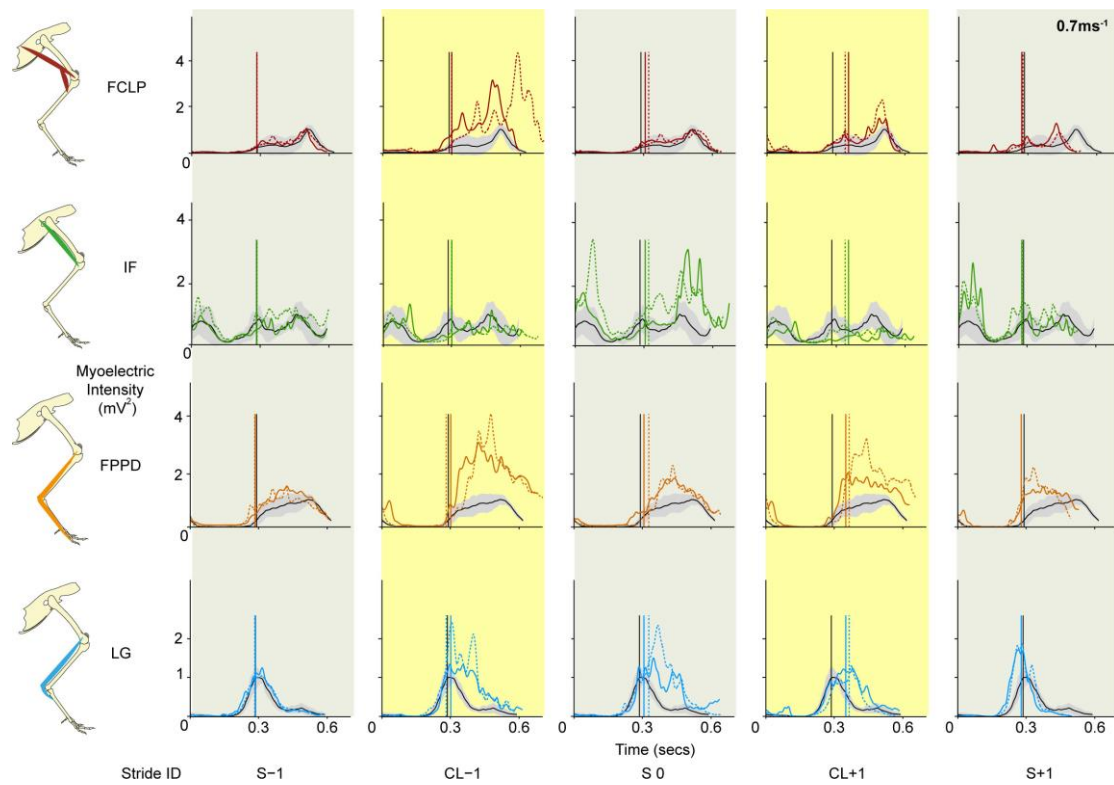
Figure 6. Average trajectories of muscle activation during slower speed obstacle negotiation, for 4 hindlimb muscles. Stride sequence as shown in **Fig. 3**. Traces are grand means of myoelectric intensity as a function of time, shown for mid-flat stride (black with grey 95% confidence interval), low contrast obstacle strides (solid coloured lines), and high contrast obstacle strides (dashed coloured lines). Vertical lines indicate toe down time (solid black for level, solid coloured for low contrast, and dashed coloured for high contrast obstacles). We show 4 muscles here to represent the main patterns observed across the limb, see **Fig. S1** for remaining muscles.
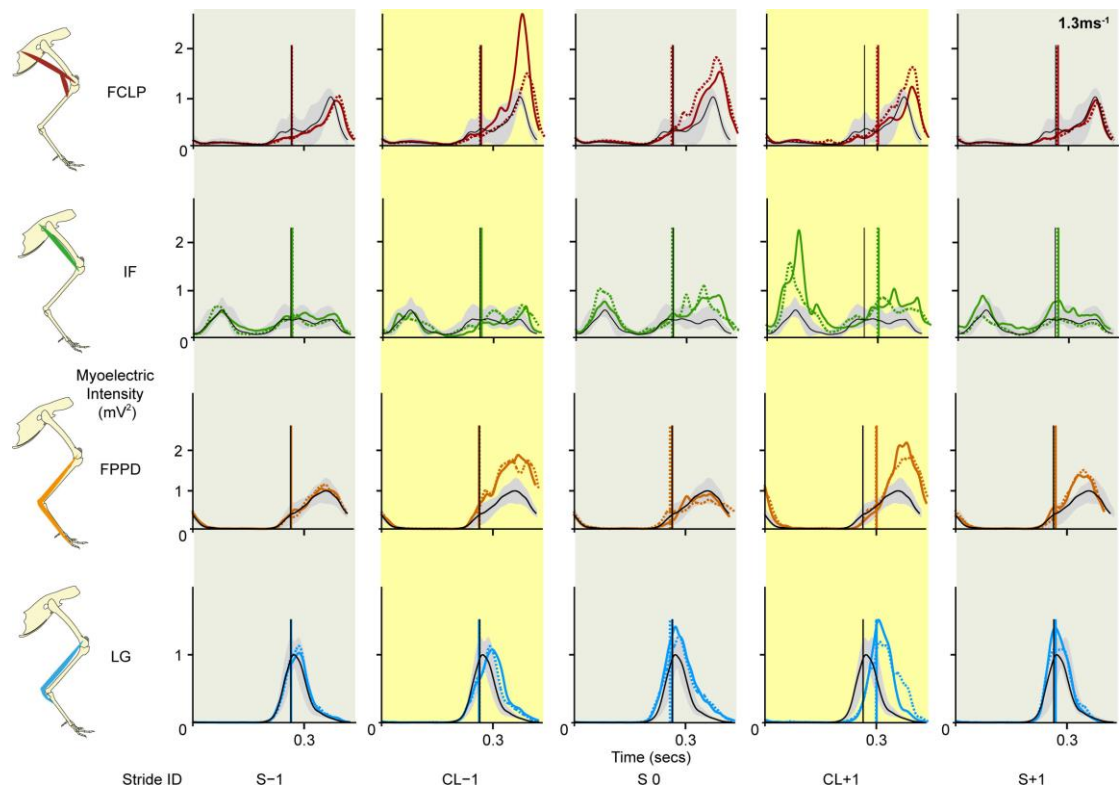
Figure 7. Average trajectories of muscle activation during higher speed obstacle negotiation, for 4 hindlimb muscles. Colours and lines as in **Fig. 6** see **Fig. S2** for remaining muscles.
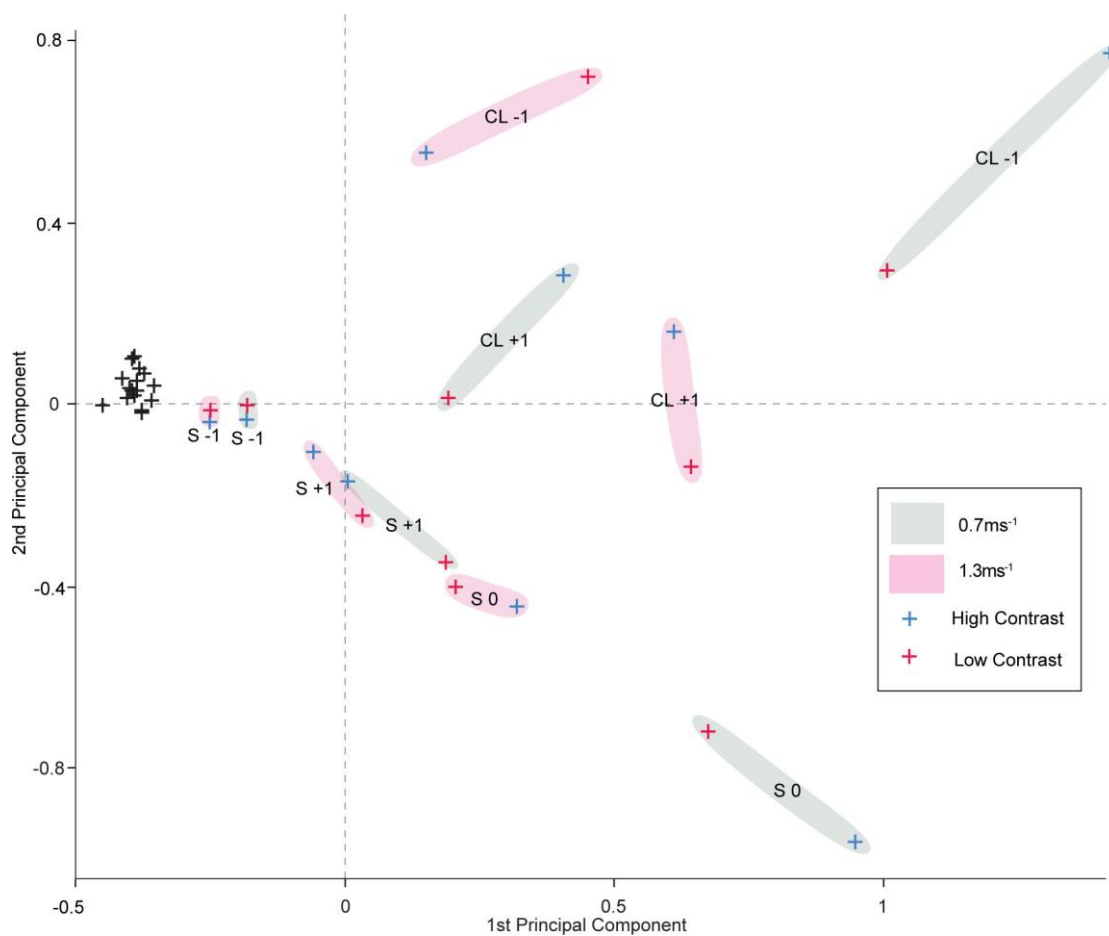
Figure 8. Principal component analysis of variance in E_{tot} across 8 hindlimb muscles and all measured terrain conditions. Scores for the first two principal components explain 85% of the variance in E_{tot} across muscles, terrains and stride categories, indicating high covariance of limb muscle activity. Scores for PC1 (horizontal axis) are shown against PC2 (vertical axis), for each stride category, with black '+' for level terrain and mid-flat strides, blue '+' for high and red '+' for low contrast obstacle strides, respectively. Shaded regions indicate clusters associated with speed and stride ID, illustrating speed-specific differences in obstacle negotiation strategy, but relatively lower variance associated with obstacle contrast. See text for further detail.
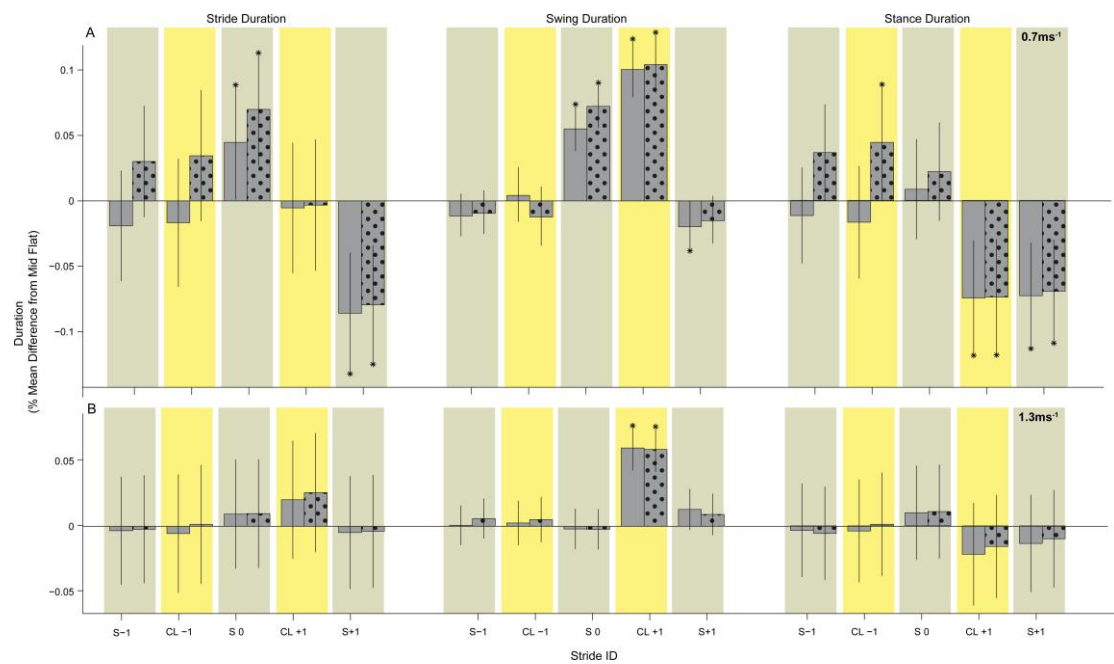
Figure 9. Changes in kinematic timing: stride duration (left), swing duration (middle) and stance duration (right), during obstacle negotiation. Stride sequence as shown in **Fig. 3**, with solid and dotted bars for low and high contrast obstacles, respectively. Bars indicate grand mean difference from mid-flat strides, with error bars indicating s.e.m. and asterisks for statistically significant posthoc pairwise differences from mid flat strides (p < 0.05).
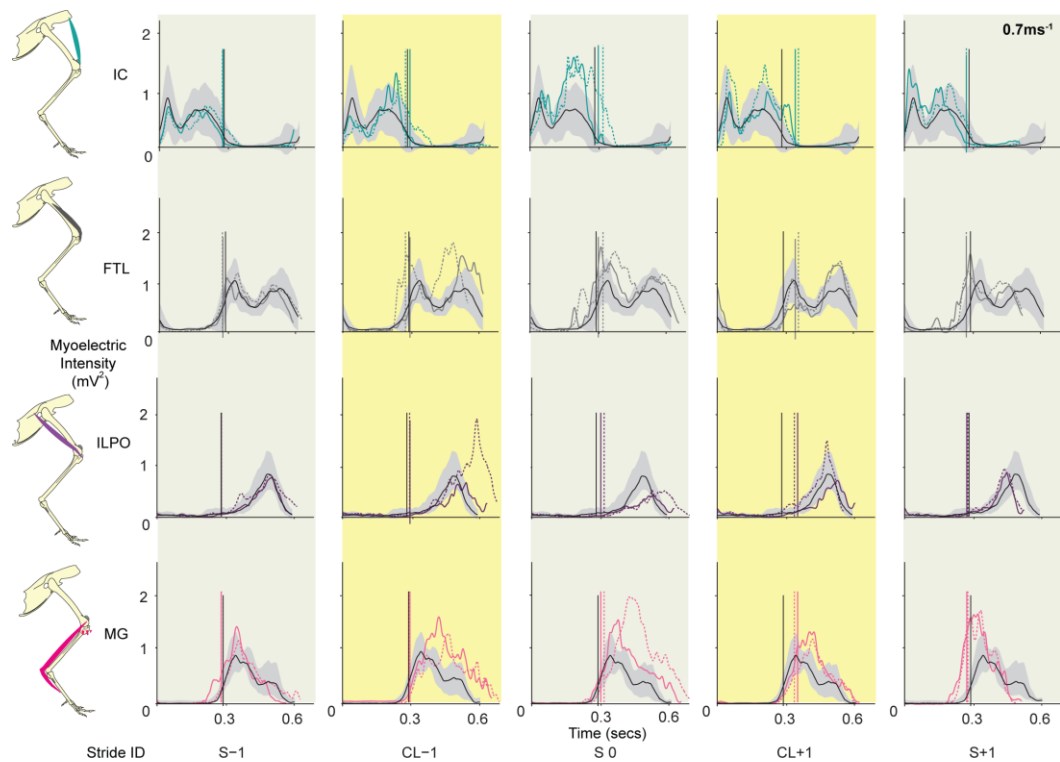
Figure S1. Average trajectories of muscle activation during the slower speed obstacle treadmill condition, for the 4 hindlimb muscles not included in Fig. 6. Stride sequence as shown in **Fig. 3**. Traces are grand means of myoelectric intensity as a function of time for each stride, shown for mid-flat stride mean (black with grey 95% confidence interval), low contrast obstacle strides (solid coloured lines), and high contrast obstacle strides (dashed coloured lines). Vertical lines indicate toe down time (solid black for level, solid coloured for low contrast, and dashed coloured for high-contrast obstacles).

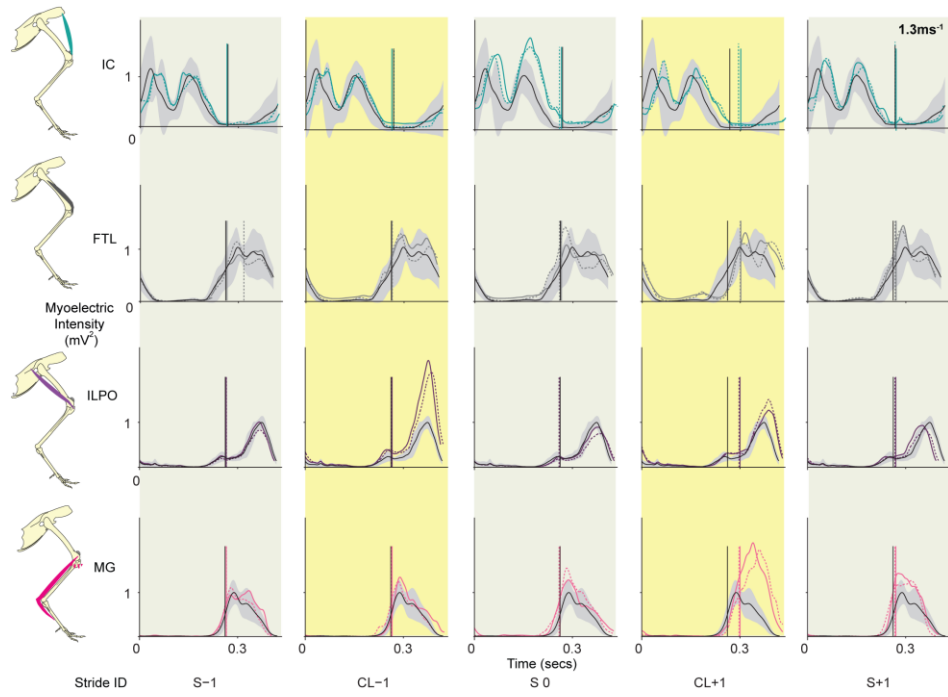**Figure S2. Average trajectories of muscle activation during the higher speed obstacle treadmill condition, for the 4 hindlimb muscles not included in Fig. 7.** Colours and lines as in **Fig. S1** legend.
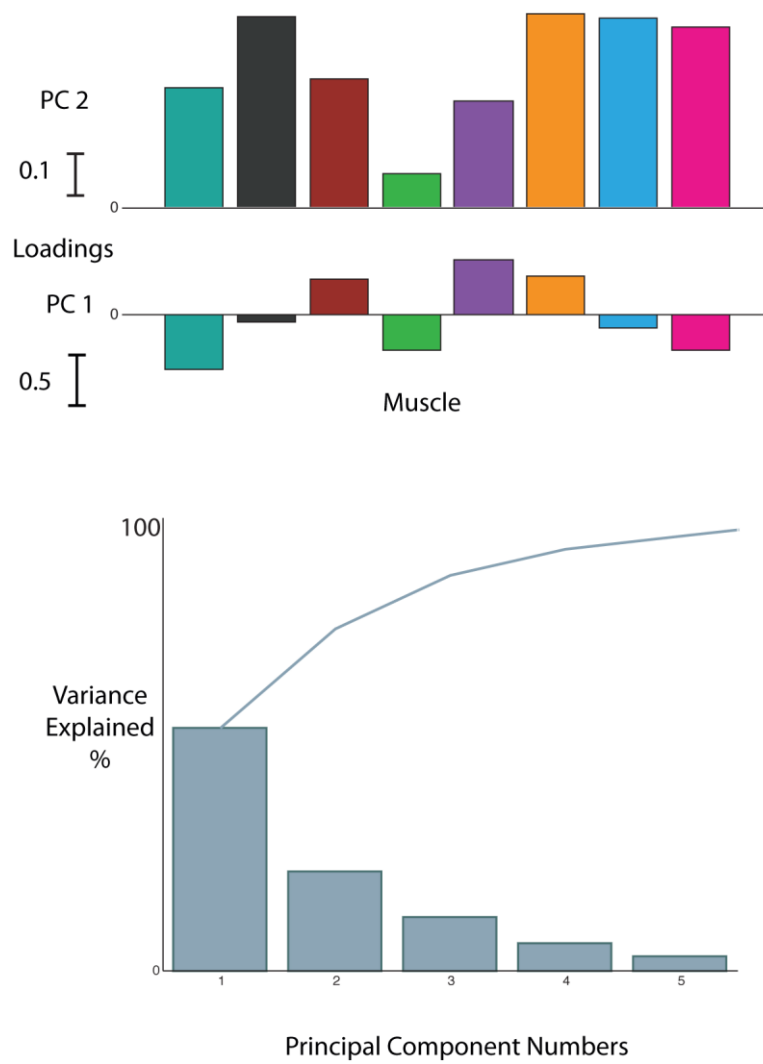
Figure S3. PCA component additional summary. Muscle weightings summarized for first two principal components (top). Percentage variance explained by first five principal components (bottom).

Table S1. Posthoc pairwise mean differences between obstacle negotiation strides and mid flat strides, at the slower treadmill speed. Statistically significant ($p \leq 0.05$) Tukey's posthoc pairwise comparisons between non-level and level strides are indicated in bold. L – low contrast obstacles. H – high contrast obstacles.

Slower speed: 0.7ms⁻¹					
Stride ID	S-1	CL-1	S 0	CL 1	S 2
IC					
L	-0.022	0.685	**0.257**	0.109	0.242
H	-0.055	0.945	**0.153**	**0.086**	0.472
FTL					
L	0.127	**0.863**	**0.333**	0.484	0.183
H	0.151	**0.906**	**0.202**	0.603	0.165
FCLP					
L	-0.001	**0.156**	0.032	1.444	0.367
H	0.150	**-0.134**	-0.370	2.135	0.385
IF					
L	-0.084	0.426	**0.119**	-0.026	-0.435
H	0.118	0.675	**0.195**	-0.186	-0.453
ILPO					
L	0.005	**-0.107**	0.073	0.715	0.113
H	0.130	**0.085**	0.156	1.086	0.559
FPPD3					
L	**0.354**	**0.604**	**0.429**	**2.190**	**1.170**
H	**0.267**	**0.557**	**0.439**	**1.872**	**1.535**
LG					
L	0.196	**1.092**	**0.318**	**0.847**	0.833
H	0.212	**1.653**	**0.544**	1.627	**0.060**

MG					
L	0.174	**0.688**	**0.603**	0.694	**0.606**
H	0.121	1.270	**0.536**	0.410	**0.260**

Table S2. Posthoc pairwise mean differences between obstacle negotiation strides and mid flat strides, at the faster treadmill speed. Statistically significant ($p \leq 0.05$) Tukey's posthoc pairwise comparisons between non-level and level strides are indicated in bold. L – low contrast obstacles. H – high contrast obstacles.

Faster speed: $1.3ms^{-1}$					
Stride ID	S-1	CL-1	S 0	CL 1	S 2
IC					
L	0.019	0.468	**0.177**	-0.017	0.011
H	-0.001	0.508	**0.110**	-0.001	0.032
FTL					
L	-0.068	0.117	0.131	0.292	0.384
H	-0.072	0.106	0.073	0.124	0.201
FCLP					
L	-0.094	**0.481**	-0.085	0.956	0.154
H	-0.054	0.960	**-0.074**	0.504	0.598
IF					
L	0.117	0.659	**0.392**	**0.178**	**1.037**
H	0.144	0.866	**0.132**	**0.257**	0.793
ILPO					
L	0.186	0.121	0.040	0.497	0.342
H	0.175	0.161	0.108	0.428	0.620
FPPD3					
L	0.049	**0.001**	0.202	**0.993**	0.874
H	0.064	**0.033**	0.272	**0.942**	**0.908**
LG					
L	0.045	0.749	**0.315**	**0.331**	0.475
H	0.119	0.753	**0.306**	**0.237**	0.624

MG					
L	0.279	0.507	**0.510**	**0.308**	**1.172**
H	0.075	0.498	**0.374**	**0.132**	0.898